assessed by echocardiographic measurements of LV ejection fraction and LV end diastolic and end systolic diameter and histopatholical measurements of myocardial fibrosis, apoptosis and myocyte cross sectional area. For the Tempol treatment group, 4-hydroxy-2,2,6,6-tetramethyl-piperidine-1-oxyl (Tempol, Sigma) was administered to AC5 Tg mice by dissolving it in drinking water at a concentration of 1mmol/L for 1 month prior to chronic ISO infusion to block oxidative stress. Animals used in this study were maintained in accordance with the Guide for the Care and Use of Laboratory Animals (National Research Council, Eighth Edition 2011). This study was approved by the Animal Care and Use Committee at New Jersey Medical School.

Experimental procedures

All techniques are described in more detail in Supplemental materials with references to previous work with these techniques. Experimental procedures included: adenoviral construction (Figure S2), physiological studies,[10] primary culture of neonatal rat ventricular myocytes,[18] AC assay,[10] immunoprecipitation, western blotting,[1] quantitative RT-PCR,[18] 8-hydroxy-2'-deoxyguanosine (8-OHdG) ELISA assay, chemiluminescent assay for superoxide production,[19] subcellular fractionation, luciferase activity, Chromatin Immunoprecipitation (ChIP) assay[15] and histological analyses (apoptosis, fibrosis and cell size).[20]

Statistical analysis

Normally distributed data were presented as mean±SEM. Otherwise, data were summarized using the Median and range. When the data were normally distributed, we used Student's unpaired t-test to compare two independent groups; otherwise, the difference was tested using the Mann-Whitney U test. For a comparison of three or more groups, one-way ANOVA was used if the sample population was normally distributed and within-group variances were approximately equal. The Student-Newman-Keuls test was used for post-hoc analysis. For data that did not meet the ANOVA assumptions, the Kruskal-Wallis test was applied and post hoc testing was carried out using the Mann-Whitney U test with Bonferroni correction. The Bonferroni correction factor is 3 for Figures 1, 5F and 5G. GraphPad-Prism 5.0 (GraphPad-Software, San Diego,CA), SPSS 20.0 (SPSS Inc, Chicago, IL) and SAS 9.3 (SAS, Research Triangle, NC) were used to perform the statistical analyses. P-values less than 0.05 defined statistical significance.

Results

AC5 Tg Mouse Model and Cardiomyopathy Induced by Chronic Isoproterenol (ISO)

AC5 protein expression, assessed by western blot analysis, was increased 26-fold in AC5 Tg (Figure S1A). Basal AC activity was increased 13-fold in AC5 Tg mice hearts compared to WT, and was increased 10-fold with forskolin compared to WT (Figure S1B). The AC5 Tg exhibited increased left ventricular ejection fraction (LVEF), p=0.0009, without ISO (WT=73(67–74)%; AC5 Tg=78(75–81)%) and heart rate was not significantly different, p=0.3176, (WT=337(325–465) bpm; AC5 Tg= 442(355–500)bpm). The increase in LVEF in response to an ISO challenge was similar in AC5 Tg and WT mice(Figure S1C).

Chronic ISO infusion induced more severe cardiomyopathy in AC5 Tg compared with WT, i.e., LVEF was lower, p=0.0058, in AC5 Tg (45(30–49)%) compared to WT (54(47–58)%). Actually the decline in LVEF was even more significant, since that takes into account the different baseline levels where LVEF was higher in AC5 Tg and fell to a lower level, p=0.0021 (Figure 1A). In addition, the LV dilated more in AC5 Tg mice than WT (Table S1). Similarly, chronic ISO induced more fibrosis (2.0-fold) and more myocyte apoptosis (2.8-fold) in AC5 Tg mice compared with WT (Figure 1B and 1C). There was also more LV

hypertrophy, as measured by myocyte cross sectional area, but the increase (1.2-fold) was not as great as with fibrosis and apoptosis.

Overexpression of AC5 Increased Oxidative Stress

After chronic ISO stimulation, AC5 Tg mice exhibited 19% more GSSG content, an indicator of oxidative stress, than WT littermates (Figure 2A). Consistent with this, AC5 Tg mice had 15% more oxidative stress-induced DNA damage compared with WT mice after chronic ISO stimulation detected by 8-OHdG ELISA (Figure 2B). In AC5 overexpressed neonatal myocytes, superoxide production was approximately 2-fold more than in the control group (Figure 2C). AC5 knockdown (KD) myocytes increased cell survival with H_2O_2 treatment (Figure 2D). MnSOD is part of a mechanism that might be responsible for the opposite response of AC5 overexpressed (OE) and AC5 KD towards oxidative stress, since MnSOD is up-regulated in AC5 KO mice.

AC5 Down-Regulates MnSOD

By western blotting, the protein expression of MnSOD was reduced 38% in AC5 Tg mice compared with WT (Figure 3A). On the cellular level, 26% less MnSOD was detected in AC5 OE myocytes and MnSOD protein was increased a 2-fold and mRNA a 3.6-fold in AC5 KD myocytes (Figure 3B, 3C and 3D). The data demonstrated that AC5 regulated the protein and mRNA expression level of MnSOD, which altered MnSOD function.

MnSOD Overexpression Ameliorated Chronic ISO Cardiomyopathy in AC5 Tg

We increased MnSOD in AC5 Tg using a bigenic (AC5 Tg × MnSOD Tg) mouse. The cardiac specific MnSOD Tg mice had a 20-fold increase in SOD activity in the heart.[21] Baseline LVEF was similar in AC5 Tg × MnSOD Tg mice (85(84–89)%) and AC5 Tg mice (78(75–81)%). After chronic ISO, the LVEF of bigenic mice decreased significantly less (Figure 1A, Table S1), p=0.0033, to 74(66–77)%, than in AC5 Tg (45(30–49)%) mice (Figure 1A, Table S1). The increases in LVEDD and LVESD were also no longer greater than observed in WT (Table S1), and the increases in fibrosis and apoptosis, observed in AC5 Tg on chronic ISO, were no longer observed in the bigenic mice (Figure 1B and 1C). Similarly, Tempol, which also protects against oxidative stress, rescued the adverse effects of the AC5 Tg after chronic ISO stimulation, i.e., the LVEF in AC5 Tg with ISO and Tempol (63(43–69)%) was higher than with ISO in AC5 Tg without Tempol (45(30–49)%). Thus, these data demonstrated that down-regulation of MnSOD in AC5 Tg mice is a key mechanism mediating the exacerbated cardiomyopathy induced by chronic ISO.

Down-regulation of MnSOD Eliminated Protective Effects of AC5 KO under Chronic Catecholamine Stress

To investigate whether MnSOD was important for the protective effects of AC5 KO mice, we crossed the AC5 KO mice with MnSOD heterozygous KO mice. Previously, we reported that the AC5 KO mice were protected against catecholamine stress.[10] This was confirmed in the present study in a small cohort, where the fall in LVEF was less in the AC5 KO than WT with chronic ISO. This protection was lost in the bigenic mice, where LVEF after chronic ISO was decreased to 50(43–60)% (n=6), which was almost identical to the LVEF in the WT mice (53(39–62)%, n=11) (Table S1). Fibrosis, an indicator of the cardiomyopathy with chronic ISO was increased similarly in WT (2.69(1.64–3.84)%) and AC5 KO × $MnSOD^{+/-}$ mice (2.92(2.32–3.85)%) compared with AC5 KO mice with chronic ISO (1.13(0.81–1.37)%).

AC5 Regulated MnSOD Transcriptionally through the SIRT1/FoxO3a Pathway

Since down-regulation of MnSOD is the key mechanism mediating the enhanced cardiomyopathy of AC5 Tg mice, we investigated the molecular pathway responsible. The mRNA level of MnSOD in AC5 KD myocytes was 3.6-fold higher than those infected by a control adenovirus, Ad-LacZ (Figure 3D), which suggested that transcriptional factors may be involved in the regulation of MnSOD, with FoxO3a a likely target, as noted earlier. To determine whether FoxO3a directly regulated MnSOD, we first examined the localization of FoxO3a in the AC5 KD neonatal myocytes. Immunostaining and western blotting detected more FoxO3a in the nucleus of AC5 KD myocytes compared with the control group (Figure 4A and 4B). Similarly in tissue, more FoxO3a was detected in the nucleus of AC5 KO mouse heart compared with WT (Figure 4C).

Next, we tested the transcriptional activity of FoxO3a using a luciferase assay by transfecting a FoxO3a luciferase vector, with a promoter containing 3 repeats of the forkhead response element (FRE), into neonatal myocytes.[22] When AC5 was knocked down in myocytes, a 2.5-fold increase in luciferase activity was observed (Figure 4D). To examine whether FoxO3a increased the native MnSOD gene directly, we performed the ChIP assay on native MnSOD in the H9C2 rat cardiac myoblast cell line infected with Ad-LacZ and Ad-shAC5, respectively. We found 1.9-fold more FoxO3a binding to the specific FoxO-binding element within the MnSOD promoter region (Figure 4E) in AC5 KD myocytes. The data demonstrated that knock down of AC5 causes FoxO3a to localize to the nucleus and associate with the MnSOD promoter.

FoxO is known to be regulated by acetylation, a modification removed by the NAD^+-responsive, metabolic sensor SIRT1.[23] To test whether AC5 regulated SIRT1 directly; protein expression of SIRT1 was detected in AC5 KO mice hearts. SIRT1 was significantly up-regulated in AC5 KO mice hearts (Figure 5A). Consistent with the adult heart data, SIRT1 was up-regulated in AC5 KD myocytes and down-regulated in AC5 OE neonatal myocytes (Figure 5C).

To test whether this pathway was unique to AC5, we also examined AC6 KO, the other major cardiac AC isoform. In AC6 KO, SIRT1 was not up-regulated (Figure 5B). Paralleling SIRT1 expression, MnSOD was not up-regulated in the AC6 KO hearts. Thus, the up-regulation of SIRT1 and MnSOD expression was not due to a general response to AC activity.

Given the apparent link between SIRT1 and FoxO3a, we found that the level of acetyl-FoxO3a in the heart of AC5 KO and AC5 Tg mice correlated inversely with the expression of SIRT1 (Figure 5D). In AC5 KD myocytes, SIRT1 was shown by co-immunoprecipitation (IP) to bind directly to FoxO3a (Figure 5E). These data suggest that FoxO3a is regulated by deacetylation in cardiac tissue and this is controlled by AC5 activity. To further investigate the role of SIRT1, we treated AC5 KD and the control group with nicotinamide, a sirtuin inhibitor, and then tested the transcriptional activity of FoxO3a in the control group. Nicotinamide did not change the activity in the control group, but reduced the transcriptional activity of FoxO3a to almost the same level in AC5 KD group as in the control group (Figure 5F). To investigate if the elevation of luciferase activity of FoxO3a contributed to MnSOD expression, we determined MnSOD protein levels in AC5 KD myocytes. The MnSOD level in nicotinamide treated AC5 KD myocytes was down-regulated to a similar level as the control group (Figure 5G). These data indicate that the increased transcriptional activity of FoxO3a and MnSOD expression in AC5 KD myocytes is due to increased SIRT1 activity. In summary, AC5 inhibited SIRT1 activity, which consequently decreased the interaction between SIRT1 and FoxO3a, thus decreasing MnSOD expression, resulting in less tolerance towards stress (Figure 6).

MnSOD also Regulated by MEK/ERK Signaling

We previously reported that both MEK/ERK/MnSOD and Akt pathways were involved in the protective mechanism of AC5 KO.[1, 10] The elevation of MnSOD in myocytes infected with AC5 KD adenovirus was eliminated by both the MEK inhibitor (PD98059)(Figure S3B) and sirtuin inhibitor (nicotinamide) (Figure 5G), suggesting both the MEK/ERK and SIRT1/FoxO3a pathway are involved in MnSOD regulation. Furthermore, we examined the activity of Akt (represented as p-Akt/Akt) in AC5 Tg mice after chronic ISO. In contrast to AC5 KO mice, the activity of Akt was lower in AC5 Tg than in WT mice (Figure S4), indicating that the AC5 Tg failed to activate this protective mechanism induced by chronic ISO stress. Different from MnSOD basal regulation by AC5 (Figure S3A), Akt is involved in mediating the cardiac effects after chronic ISO stimulation.

To demonstrate that MnSOD is the only anti-oxidant gene targeted by the AC5 regulated Sirt1/FoxO3a pathway, we examined the expression of catalase, another downstream target of FoxO3a,[24, 25] and found no differences in the hearts among WT, AC5 KO and AC5 Tg mice (Figure S5).

Discussion

Since the conclusions from previous studies examining the extent to which cardiac overexpression or deletion of AC5 affects the development of cardiomyopathy have been controversial[6, 7, 17, 26] and no prior study examined the effects of cardiac overexpression of AC5 on the development of cardiomyopathy, the goal of the present investigation was to do just that, using the model of chronic catecholamine stress. The results indicate clearly that cardiac over-expression of AC5 increases the severity of the cardiomyopathy induced by chronic catecholamine stress, resulting in more severely compromised LV function and increased LV dilation, cardiac fibrosis and apoptosis. It is well recognized that catecholamines increase oxidative stress, which in turn, induces necrosis and results in cardiac fibrosis,[27–30] which is an important mechanism mediating the decrease in function observed, not only in the cardiomyopathy induced by chronic ISO, but also in all cardiomyopathies. Although the most common cause of necrosis is myocardial ischemia, it can also result from an imbalance between myocardial oxygen supply and demand, particularly in the subendocardium, and there is also non-ischemic necrosis,[27] all of which leads to a reduction in contractile units in the heart and increased fibrosis, which interferes with cardiac contraction. ISO also induces necrosis in myocytes in culture, independent of myocardial blood supply.[27, 31, 32]

There is another reason for controversial results in literature, i.e., it is not always possible to extrapolate linearly between in vivo and in vitro work and between Tg and KO models. A major strength of this investigation was the use of both Tg and KO models for AC5, which alleviated the criticisms that the high level of overexpression of AC5 in the Tg model, overwhelmed other mechanisms. In addition, finding reciprocal data in the KO and Tg model strengthens the conclusions.

Since MnSOD protects against oxidative stress in AC5 KO mice[1] and since oxidative stress has been implicated in catecholamine induced cardiomyopathy,[11, 27, 33] our hypothesis was that the adverse effects of AC5 overexpression in the heart are mediated by enhanced oxidative stress, primarily through an MnSOD mechanism. Confirming this hypothesis we found a 36% decrease of MnSOD expression in AC5 Tg mice and greater oxidative stress induced DNA damage. To further confirm our hypothesis that the reduced MnSOD was responsible for the enhanced oxidative stress, we restored MnSOD to the AC5 Tg mice by mating them with MnSOD Tg mice. The bigenic mice no longer responded to chronic ISO with more severe cardiomyopathy. To further confirm our hypothesis, we also examined

whether reducing MnSOD eliminated the protection afforded to AC5 KO mice. Accordingly, we also mated $MnSOD^{+/-}$ mice with AC5 KO mice and then subjected the bigenic mice to chronic ISO stimulation. The bigenic mice were no longer protected from chronic catecholamine stress. Thus, the level of expression of MnSOD was responsible for the difference in responses to chronic catecholamine stimulation from WT in AC5 Tg and AC5 KO mice, and the opposite responses in AC5 Tg and AC5 KO mice. It was important to use the KO model in parallel with the AC5 Tg model, to avoid complicating influences derived from increasing gene expression to a high level. More importantly, the elimination of the protective effect in AC5 KO × $MnSOD^{+/-}$ mice is direct evidence that indicates the importance of MnSOD in the AC5 regulatory pathway. Other studies have found that oxidative stress is an important mechanism mediating several different cardiomyopathies,[28–30, 33, 34] and Dai et al., showed the importance of mitochondrial oxidative stress.[35] However, the signaling pathways have not been elucidated.

In this connection, it was previously shown that impaired mitochondrial function in cardiac myocytes from $Sod2^{+/-}$ mouse hearts is associated with a reduction in MnSOD activity[36], which might suggest that the same phenomenon might occur in the AC5 Tg, where MnSOD activity is reduced, and that this may reduce cardiac function. However, we observed increased LV function at baseline in AC5 Tg and impaired function with chronic ISO. This apparent conundrum can be explained by the complex interaction of mechanisms controlling cardiac function in normal animals in vivo and more so in Tg animals. Since AC5 is a direct downstream target of the beta-AR, the increased basal LV function is a result of amplifying signals from the beta-AR, and not due to reduced MnSOD expression. Chronic ISO stress in AC5 Tg leads to the accumulation of oxidative stress, and an imbalance between oxygen supply and demand in the heart, leading to necrosis, apoptosis and fibrosis, which consequently reduced LV function and resulted in cardiomyopathy.

We then investigated the signaling pathway by which AC5 regulated MnSOD expression. In AC5 KD myocytes, we detected a significant increase in MnSOD mRNA, which suggests that AC5 also regulated MnSOD in a transcriptional manner. As noted earlier, the experiments demonstrating the role of MnSOD in mediating the enhanced cardiomyopathy with chronic ISO stress in AC5 Tg led us to investigate the SIRT1/FoxO3a pathway, in view of its protective role against oxidative stress associated with aging in *C. elegans*,[13, 14] rats[15] and human quiescent cells.[16] In our study, we demonstrate for the first time the importance of AC5, an up-stream gene of the SIRT1/FoxO3a complex regulating MnSOD in cardiomyopathy. We also found activation of SIRT1 and FoxO3a in AC5 KD myocytes, whereas inhibition was detected in AC5 OE myocytes, suggesting that AC5 inhibits SIRT1 and FoxO3a activity, resulting in an impaired anti-oxidant system and induced cell death, suggesting that overexpression of SIRT1 and/or nicotinamide mononucleotide (NMN) or nicotinamide riboside treatment[37] should be able to counteract the adverse effects of increased AC5 in the setting of chronic catecholamine cardiomyopathy. These conclusions are based in part on the acetylation experiments, which have the limitation of using the immunoprecipitation technique.[38] A future direction will be to utilize a specific antibody for acetyl FoxO3a when it is available, which would permit a more definitive conclusion.

FoxO3a is known to regulate MnSOD transcriptionally, protecting cells from cellular oxidative stress.[16] FoxO activity is regulated, in turn, by SIRT1, which also exerts favorable effects on oxidative stress resistance in cardiac myocytes.[23] An interaction between the cyclic AMP/PKA pathway and Sir2 (an ortholog of SIRT1) in yeast has been reported.[39] Recently a few studies indicated cyclic AMP/PKA dependent pathways of SIRT1 activation,[40,41] which seem to be at variance with our findings. However, there are at least 4 important differences between these studies and ours. These studies were conducted in cancer, skeletal muscle, or hepatic cells, whereas we examined cardiomyocytes. Secondly,

our findings are related only to AC5; it is conceivable that other AC isoforms, even AC6, the other major isoform in the heart could induce different regulation. Indeed, this is what we observed. Since in the studies by Noriega and Gerhart-Hines, forskolin was used to stimulate AC, which will activate all AC isoforms, this may have influenced AC6, which regulates AC activity to a greater effect than AC5 in the heart. Fourthly, our study was conducted under conditions of chronic activation or inhibition of the cyclic AMP/PKA pathway, e.g., in AC5 Tg and KO, and measured the change in protein expression of SIRT1, whereas the prior studies utilized more acute activation of cyclic AMP/PKA with forskolin, which activated SIRT1, either through the induction of its transcription or through SIRT1 phosphorylation. Finally, the results of our investigation relating AC5 to the SIRT1/FoxO pathway is consistent with other studies showing that SIRT1/FoxO protects the heart against oxidative stress, and that MnSOD plays an important role.[42, 43] It has been shown that overexpression of SIRT1 no longer promotes cell survival when MnSOD was eliminated[42] and nuclear translocation of FoxO induced transcriptional up-regulation of MnSOD, which protected the heart from myocardial infarction.[43] In addition, we found translocation and activation of FoxO3a by SIRT1, consistent with a report in *C. elegans*.[23] Since FoxO3a regulates several molecules involved in the cell cycle and oxidative stress, e.g., catalase[24, 25] it is possible that MnSOD is not uniquely targeted. However, we found that catalase expression was not different in hearts from WT, AC5 Tg and AC5 KO (Figure S5), supporting the concept that MnSOD is uniquely regulated by FoxO3a with relation to AC5. Deacetylation of FoxO3a should activate the transcriptional activity as described previously.[23] As shown in Figure 5F and 5G, inhibition of SIRT1 activity reduced the FoxO3a transcriptional activity and MnSOD expression in AC5 KD myocytes. Since MnSOD is one of the important down-stream targets of FoxO3a, it is expected that the binding affinity to the MnSOD promoter increases as FoxO3a is activated.

It is important that we found the signaling mechanisms differed in the two major cardiac AC isoforms, AC5 and AC6. There have been several instances of AC isoform differences within organs. AC1, AC5, and AC8 all are major isoforms in brain, AC1 and AC8 play an important role in memory and learning,[44, 45] but not AC5. Similarly, AC1 KO and AC5 KO mice are resistant to pain stress,[46, 47] but not AC8. Also there are apparent differences in AC5 and AC6 regulation in the heart, showing that the AC5 KO is protected against stress,[9, 10] but not AC6 KO.[48]

We previously found that the MEK/ERK pathway regulated MnSOD in the AC5 KO.[1] In the current investigation we found that MnSOD was upregulated similarly in AC5 KO mice with vehicle and with ISO (Figure S3A) and that both a MEK inhibitor and a sirtuin inhibitor blocked the elevation of MnSOD in AC5 KD myocytes (Figure S3B, 5G), suggesting that both of these pathways are involved in the regulation of MnSOD by AC5.

In summary, this study examined for the first time the effects of overexpression of AC5 on the response to cardiac stress. In contrast to conflicting results from prior studies in AC5 Tg,[6, 7] the results of the current investigation indicate clearly that overexpression of AC5 is deleterious in response to cardiac stress. We also demonstrated a new pathway for cardiac dysfunction mediated by AC5; cardiac overexpression of AC5 exacerbates the cardiomyopathy induced by chronic catecholamine stress through a mechanism inhibiting SIRT1 and FoxO3a, which decreases MnSOD transcription. The impaired antioxidant system elevates the intercellular oxidative stress level with chronic ISO stimulation, inducing more cell death and resulting in augmented cardiac dysfunction.

Supplementary Material

Refer to Web version on PubMed Central for supplementary material.

Acknowledgments

We appreciated the generous gifts of the MnSOD$^{+/-}$ mouse model by Dr. Ting-Ting Huang. We thank Dr. Chunbo Wang and Dr. Yimin Tian for technical support of the immunohistology analyses.

Funding Sources

This study was supported by funding from National Institutes of Health (5R01HL093481, 1R01HL106511, 5P01AG027211, 1R01HL102472, 5R01HL033107, 5T32HL069752, 5R01HL095888, 5P01HL069020, 5R01HL091781, 5R01HL093415, 5R01AG028730, 1R01AG019719). Dr. David A. Sinclair is supported by the Glenn Foundation for Medical Research.

References

1. Yan L, Vatner DE, O'Connor JP, Ivessa A, Ge H, Chen W, Hirotani S, Ishikawa Y, Sadoshima J, Vatner SF. Type 5 adenylyl cyclase disruption increases longevity and protects against stress. Cell. 2007; 130:247–258. [PubMed: 17662940]
2. Hines LM, Tabakoff B. Platelet adenylyl cyclase activity: A biological marker for major depression and recent drug use. Biological psychiatry. 2005; 58:955–962. [PubMed: 16095566]
3. El-Mowafy AM, Alkhalaf M. Resveratrol activates adenylyl-cyclase in human breast cancer cells: A novel, estrogen receptor-independent cytostatic mechanism. Carcinogenesis. 2003; 24:869–873. [PubMed: 12771030]
4. Hanoune J, Defer N. Regulation and role of adenylyl cyclase isoforms. Annual review of pharmacology and toxicology. 2001; 41:145–174.
5. Moorman C, Plasterk RH. Functional characterization of the adenylyl cyclase gene sgs-1 by analysis of a mutational spectrum in caenorhabditis elegans. Genetics. 2002; 161:133–142. [PubMed: 12019229]
6. Tepe NM, Liggett SB. Transgenic replacement of type v adenylyl cyclase identifies a critical mechanism of beta-adrenergic receptor dysfunction in the g alpha q overexpressing mouse. FEBS Lett. 1999; 458:236–240. [PubMed: 10481072]
7. Petrashevskaya N, Gaume BR, Mihlbachler KA, Dorn GW 2nd, Liggett SB. Bitransgenesis with beta(2)-adrenergic receptors or adenylyl cyclase fails to improve beta(1)-adrenergic receptor cardiomyopathy. Clin Transl Sci. 2008; 1:221–227. [PubMed: 20443853]
8. Timofeyev V, Porter CA, Tuteja D, Qiu H, Li N, Tang T, Singapuri A, Han PL, Lopez JE, Hammond HK, Chiamvimonvat N. Disruption of adenylyl cyclase type v does not rescue the phenotype of cardiac-specific overexpression of galphaq protein-induced cardiomyopathy. Am J Physiol Heart Circ Physiol. 2010; 299:H1459–H1467. [PubMed: 20709863]
9. Okumura S, Takagi G, Kawabe J, Yang G, Lee MC, Hong C, Liu J, Vatner DE, Sadoshima J, Vatner SF, Ishikawa Y. Disruption of type 5 adenylyl cyclase gene preserves cardiac function against pressure overload. Proc Natl Acad Sci U S A. 2003; 100:9986–9990. [PubMed: 12904575]
10. Okumura S, Vatner DE, Kurotani R, Bai Y, Gao S, Yuan Z, Iwatsubo K, Ulucan C, Kawabe J, Ghosh K, Vatner SF, Ishikawa Y. Disruption of type 5 adenylyl cyclase enhances desensitization of cyclic adenosine monophosphate signal and increases akt signal with chronic catecholamine stress. Circulation. 2007; 116:1776–1783. [PubMed: 17893275]
11. Zhang GX, Kimura S, Nishiyama A, Shokoji T, Rahman M, Yao L, Nagai Y, Fujisawa Y, Miyatake A, Abe Y. Cardiac oxidative stress in acute and chronic isoproterenol-infused rats. Cardiovasc Res. 2005; 65:230–238. [PubMed: 15621051]
12. Srivastava S, Chandrasekar B, Gu Y, Luo J, Hamid T, Hill BG, Prabhu SD. Downregulation of cuzn-superoxide dismutase contributes to beta-adrenergic receptor-mediated oxidative stress in the heart. Cardiovasc Res. 2007; 74:445–455. [PubMed: 17362897]
13. Lin K, Hsin H, Libina N, Kenyon C. Regulation of the caenorhabditis elegans longevity protein daf-16 by insulin/igf-1 and germline signaling. Nature genetics. 2001; 28:139–145. [PubMed: 11381260]
14. Furuyama T, Nakazawa T, Nakano I, Mori N. Identification of the differential distribution patterns of mrnas and consensus binding sequences for mouse daf-16 homologues. The Biochemical journal. 2000; 349:629–634. [PubMed: 10880363]

15. Li M, Chiu JF, Mossman BT, Fukagawa NK. Down-regulation of manganese-superoxide dismutase through phosphorylation of foxo3a by akt in explanted vascular smooth muscle cells from old rats. J Biol Chem. 2006; 281:40429–40439. [PubMed: 17079231]
16. Kops GJ, Dansen TB, Polderman PE, Saarloos I, Wirtz KW, Coffer PJ, Huang TT, Bos JL, Medema RH, Burgering BM. Forkhead transcription factor foxo3a protects quiescent cells from oxidative stress. Nature. 2002; 419:316–321. [PubMed: 12239572]
17. Hu CL, Chandra R, Ge H, Pain J, Yan L, Babu G, Depre C, Iwatsubo K, Ishikawa Y, Sadoshima J, Vatner SF, Vatner DE. Adenylyl cyclase type 5 protein expression during cardiac development and stress. Am J Physiol Heart Circ Physiol. 2009; 297:H1776–H1782. [PubMed: 19734365]
18. Qiu H, Lizano P, Laure L, Sui X, Rashed E, Park JY, Hong C, Gao S, Holle E, Morin D, Dhar SK, Wagner T, Berdeaux A, Tian B, Vatner SF, Depre C. H11 kinase/heat shock protein 22 deletion impairs both nuclear and mitochondrial functions of stat3 and accelerates the transition into heart failure on cardiac overload. Circulation. 2011; 124:406–415. [PubMed: 21747053]
19. Ago T, Kitazono T, Ooboshi H, Iyama T, Han YH, Takada J, Wakisaka M, Ibayashi S, Utsumi H, Iida M. Nox4 as the major catalytic component of an endothelial nad(p)h oxidase. Circulation. 2004; 109:227–233. [PubMed: 14718399]
20. Peter PS, Brady JE, Yan L, Chen W, Engelhardt S, Wang Y, Sadoshima J, Vatner SF, Vatner DE. Inhibition of p38 alpha mapk rescues cardiomyopathy induced by overexpressed beta 2-adrenergic receptor, but not beta 1-adrenergic receptor. The Journal of clinical investigation. 2007; 117:1335–1343. [PubMed: 17446930]
21. Shen X, Zheng S, Metreveli NS, Epstein PN. Protection of cardiac mitochondria by overexpression of mnsod reduces diabetic cardiomyopathy. Diabetes. 2006; 55:798–805. [PubMed: 16505246]
22. Brunet A, Bonni A, Zigmond MJ, Lin MZ, Juo P, Hu LS, Anderson MJ, Arden KC, Blenis J, Greenberg ME. Akt promotes cell survival by phosphorylating and inhibiting a forkhead transcription factor. Cell. 1999; 96:857–868. [PubMed: 10102273]
23. Brunet A, Sweeney LB, Sturgill JF, Chua KF, Greer PL, Lin Y, Tran H, Ross SE, Mostoslavsky R, Cohen HY, Hu LS, Cheng HL, Jedrychowski MP, Gygi SP, Sinclair DA, Alt FW, Greenberg ME. Stress-dependent regulation of foxo transcription factors by the sirt1 deacetylase. Science. 2004; 303:2011–2015. [PubMed: 14976264]
24. Nemoto S, Finkel T. Redox regulation of forkhead proteins through a p66shc-dependent signaling pathway. Science. 2002; 295:2450–2452. [PubMed: 11884717]
25. van der Horst A, Burgering BM. Stressing the role of foxo proteins in lifespan and disease. Nature reviews. Molecular cell biology. 2007; 8:440–450.
26. Iwatsubo K, Bravo C, Uechi M, Baljinnyam E, Nakamura T, Umemura M, Lai L, Gao S, Yan L, Zhao X, Park M, Qiu H, Okumura S, Iwatsubo M, Vatner DE, Vatner SF, Ishikawa Y. Prevention of heart failure in mice by an antiviral agent that inhibits type 5 cardiac adenylyl cyclase. American journal of physiology. Heart and circulatory physiology. 2012; 302:H2622–H2628. [PubMed: 22505646]
27. Khan MU, Cheema Y, Shahbaz AU, Ahokas RA, Sun Y, Gerling IC, Bhattacharya SK, Weber KT. Mitochondria play a central role in nonischemic cardiomyocyte necrosis: Common to acute and chronic stressor states. Pflugers Arch. 2012; 464:123–131. [PubMed: 22328074]
28. Robinson AD, Ramanathan KB, McGee JE, Newman KP, Weber KT. Oxidative stress and cardiomyocyte necrosis with elevated serum troponins: Pathophysiologic mechanisms. Am J Med Sci. 2011; 342:129–134. [PubMed: 21747281]
29. Ungvari Z, Gupte SA, Recchia FA, Batkai S, Pacher P. Role of oxidative-nitrosative stress and downstream pathways in various forms of cardiomyopathy and heart failure. Curr Vasc Pharmacol. 2005; 3:221–229. [PubMed: 16026319]
30. Wexler RK, Elton T, Pleister A, Feldman D. Cardiomyopathy: An overview. American family physician. 2009; 79:778–784. [PubMed: 20141097]
31. Izem-Meziane M, Djerdjouri B, Rimbaud S, Caffin F, Fortin D, Garnier A, Veksler V, Joubert F, Ventura-Clapier R. Catecholamine-induced cardiac mitochondrial dysfunction and mptp opening: Protective effect of curcumin. American journal of physiology. Heart and circulatory physiology. 2012; 302:H665–H674. [PubMed: 22101527]

32. Matzinger P. The danger model: A renewed sense of self. Science. 2002; 296:301–305. [PubMed: 11951032]
33. Dhalla NS, Adameova A, Kaur M. Role of catecholamine oxidation in sudden cardiac death. Fundam Clin Pharmacol. 2010; 24:539–546. [PubMed: 20584205]
34. Shaheen M, Cheema Y, Shahbaz AU, Bhattacharya SK, Weber KT. Intracellular calcium overloading and oxidative stress in cardiomyocyte necrosis via a mitochondriocentric signal-transducer-effector pathway. Exp Clin Cardiol. 2011; 16:109–115. [PubMed: 22131852]
35. Dai DF, Johnson SC, Villarin JJ, Chin MT, Nieves-Cintron M, Chen T, Marcinek DJ, Dorn GW 2nd, Kang YJ, Prolla TA, Santana LF, Rabinovitch PS. Mitochondrial oxidative stress mediates angiotensin ii-induced cardiac hypertrophy and galphaq overexpression-induced heart failure. Circ Res. 2011; 108:837–846. [PubMed: 21311045]
36. Van Remmen H, Williams MD, Guo Z, Estlack L, Yang H, Carlson EJ, Epstein CJ, Huang TT, Richardson A. Knockout mice heterozygous for sod2 show alterations in cardiac mitochondrial function and apoptosis. American journal of physiology. Heart and circulatory physiology. 2001; 281:H1422–H1432. [PubMed: 11514315]
37. Canto C, Houtkooper RH, Pirinen E, Youn DY, Oosterveer MH, Cen Y, Fernandez-Marcos PJ, Yamamoto H, Andreux PA, Cettour-Rose P, Gademann K, Rinsch C, Schoonjans K, Sauve AA, Auwerx J. The nad(+) precursor nicotinamide riboside enhances oxidative metabolism and protects against high-fat diet-induced obesity. Cell metabolism. 2012; 15:838–847. [PubMed: 22682224]
38. Qin W, Zhao W, Ho L, Wang J, Walsh K, Gandy S, Pasinetti GM. Regulation of forkhead transcription factor foxo3a contributes to calorie restriction-induced prevention of alzheimer's disease-type amyloid neuropathology and spatial memory deterioration. Annals of the New York Academy of Sciences. 2008; 1147:335–347. [PubMed: 19076455]
39. Lin SJ, Defossez PA, Guarente L. Requirement of nad and sir2 for life-span extension by calorie restriction in saccharomyces cerevisiae. Science. 2000; 289:2126–2128. [PubMed: 11000115]
40. Gerhart-Hines Z, Dominy JE Jr, Blattler SM, Jedrychowski MP, Banks AS, Lim JH, Chim H, Gygi SP, Puigserver P. The camp/pka pathway rapidly activates sirt1 to promote fatty acid oxidation independently of changes in nad(+). Mol cell. 2011; 44:851–863. [PubMed: 22195961]
41. Noriega LG, Feige JN, Canto C, Yamamoto H, Yu J, Herman MA, Mataki C, Kahn BB, Auwerx J. Creb and chrebp oppositely regulate sirt1 expression in response to energy availability. EMBO reports. 2011; 12:1069–1076. [PubMed: 21836635]
42. Tanno M, Kuno A, Yano T, Miura T, Hisahara S, Ishikawa S, Shimamoto K, Horio Y. Induction of manganese superoxide dismutase by nuclear translocation and activation of sirt1 promotes cell survival in chronic heart failure. J Biol Chem. 2010; 285:8375–8382. [PubMed: 20089851]
43. Sengupta A, Molkentin JD, Paik JH, DePinho RA, Yutzey KE. Foxo transcription factors promote cardiomyocyte survival upon induction of oxidative stress. J Biol Chem. 2011; 286:7468–7478. [PubMed: 21159781]
44. Wong ST, Athos J, Figueroa XA, Pineda VV, Schaefer ML, Chavkin CC, Muglia LJ, Storm DR. Calcium-stimulated adenylyl cyclase activity is critical for hippocampus-dependent long-term memory and late phase ltp. Neuron. 1999; 23:787–798. [PubMed: 10482244]
45. Wang HB, Pineda VV, Chan GCK, Wong ST, Muglia LJ, Storm DR. Type 8 adenylyl cyclase is targeted to excitatory synapses and required for mossy fiber long-term potentiation. Journal of Neuroscience. 2003; 23:9710–9718. [PubMed: 14585998]
46. Vadakkan KI, Wang HS, Ko SW, Zastepa E, Petrovic MJ, Sluka KA, Zhuo M. Genetic reduction of chronic muscle pain in mice lacking calcium/calmodulin-stimulated adenylyl cyclases. Molecular Pain. 2006:2. [PubMed: 16412244]
47. Kim KS, Kim J, Back SK, Im JY, Na HS, Han PL. Markedly attenuated acute and chronic pain responses in mice lacking adenylyl cyclase-5. Genes, brain, and behavior. 2007; 6:120–127.
48. Lai NC, Tang T, Gao MH, Saito M, Takahashi T, Roth DM, Hammond HK. Activation of cardiac adenylyl cyclase expression increases function of the failing ischemic heart in mice. J Am Coll Cardiol. 2008; 51:1490–1497. [PubMed: 18402905]

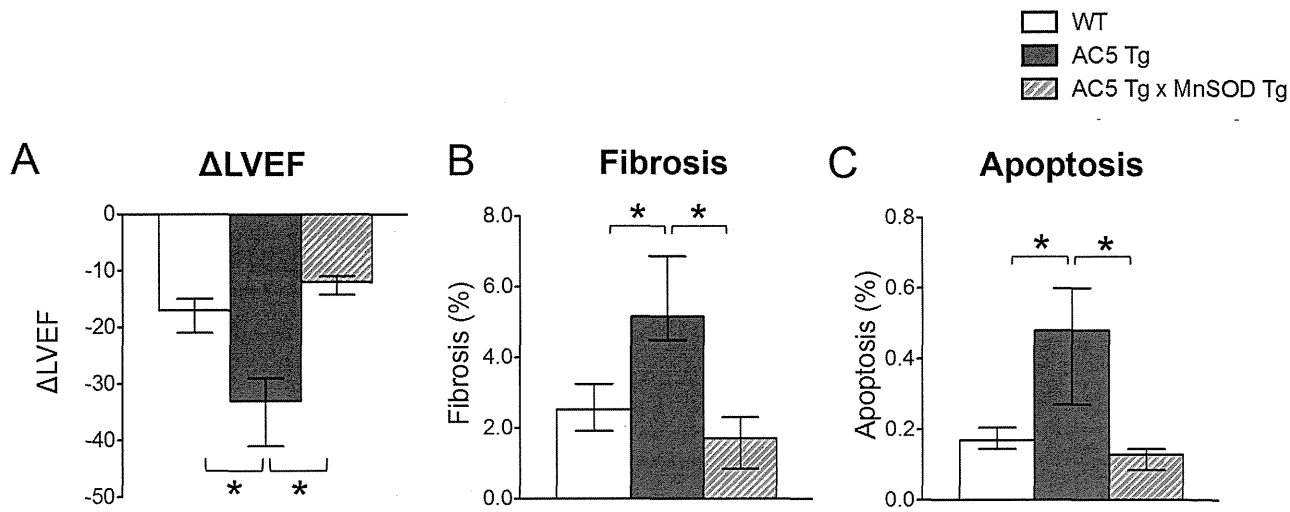

Figure 1.

Chronic ISO cardiomyopathy in AC5 Tg, compared with WT, was rescued by mating the AC5 Tg mice with MnSOD Tg (AC5 Tg × MnSOD Tg) mice. The asterix indicates a $p<0.05$ difference. **A,** Delta LV ejection fraction (EF) after ISO. AC5 Tg mice fell significantly more than that of WT mice, $p<0.05$. In the bigenic mice the fall in LVEF was significantly less, n=6–7/group. **B,** More fibrosis, $p<0.05$, was detected in AC5 Tg mice after ISO than in the other two groups after ISO n=5/group. **C,** Myocyte apoptosis, calculated by the percentage of total myocyte nuclei, also increased more in AC5 Tg than the other two groups. The data in panel **A–C** did not have a normal distribution and the appropriate statistical tests were used (see statistical analysis section). *$p<0.05$

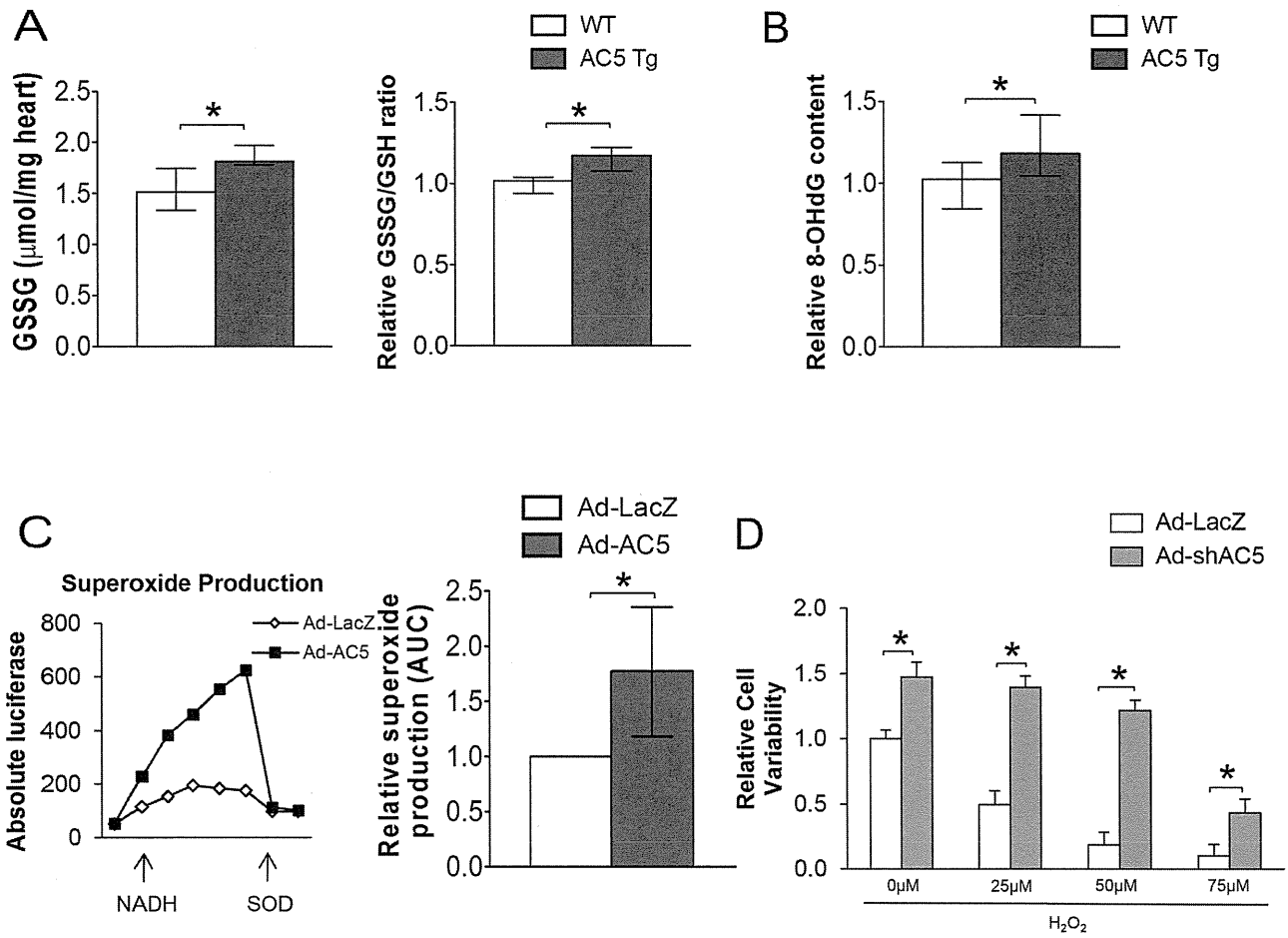

Figure 2.

Oxidative stress was detected in AC5 Tg mice. **A,** Higher GSSG content (left panel), as well as GSSG/GSH ratio (right panel) were detected in AC5 Tg heart after chronic ISO stimulation. n=5/group. **B,** The elevation of oxidative stress in AC5 Tg heart after chronic ISO stimulation was further confirmed by 8-OHdG (a marker of oxidative DNA damage) ELISA assay. n=7/group. **C,** Ad-AC5 infected myocytes released approximately 2-fold more superoxide radicals than control myocytes. n=4. **D,** Knocking down AC5 improved cell survival in myocytes treated with various concentrations of H_2O_2. n=8. The data in panels **A, B** and **C** did not have a normal distribution and the appropriate statistical tests were used (see statistical analysis section). The data in panel **D** had a normal distribution and were presented as mean±sem. *$p<0.05$ by 1-way ANOVA with Student-Newman-Keuls post-hoc analysis. *$p<0.05$

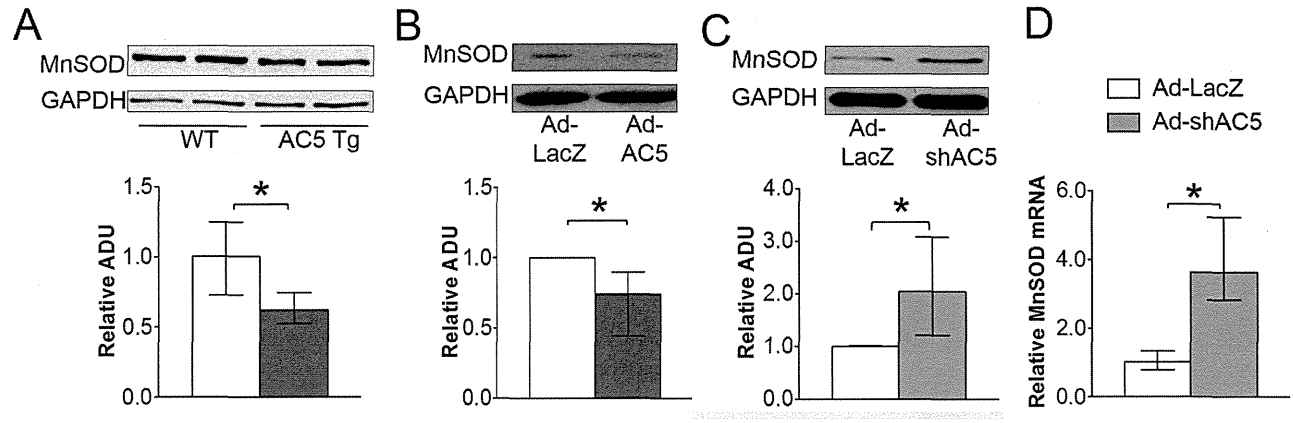

Figure 3.

AC5 regulated MnSOD expression in protein and mRNA levels. Panels **A** and **B** show the downregulation of MnSOD in AC5 Tg mice hearts (n=6/group) and Ad-AC5 infected myocytes (n=4). **C,** MnSOD was up-regulated in Ad-shAC5 infected myocytes, n=4. **D,** mRNA also increased in AC5 knock down myocytes, n=9/group. The data in panels **A – D** did not have a normal distribution and the appropriate statistical tests were used (see statistical analysis section). *$p<0.05$

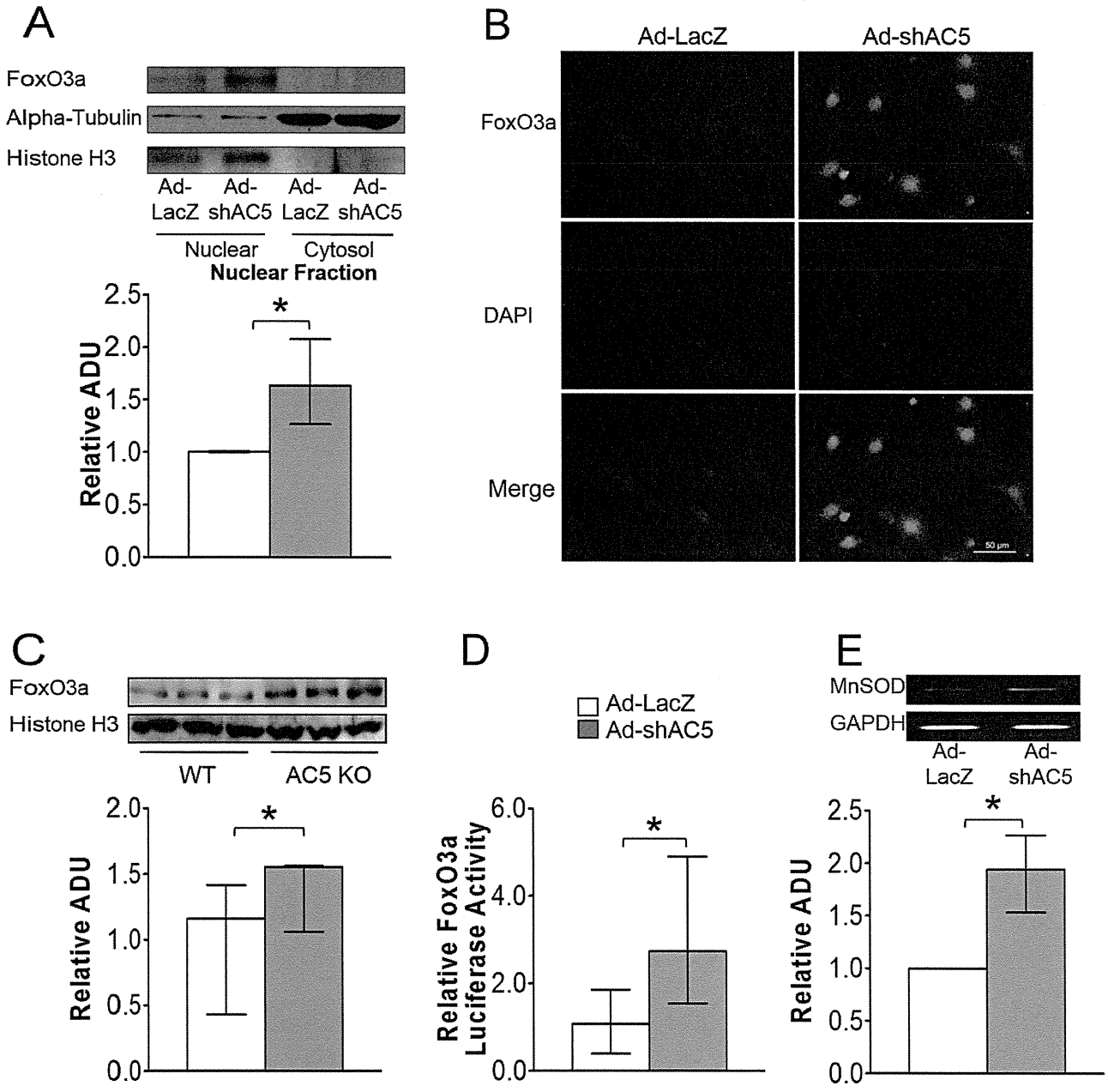

Figure 4.

AC5 regulated MnSOD transcriptionally through FoxO3a. **A** and **B**, Both immunostaining (40×) and western blotting confirm the nuclear localization of FoxO3a in AC5 KD myocytes, n=4. The data are normalized to the intensity of histone H3. **C,** More FoxO3a expression was detected in the nuclear fraction of AC5 KO heart, n=3/group. **D,** Myocytes infected with Ad-shAC5 showed significantly higher transcriptional activity compared with Ad-LacZ infected cells, n=9/group. **E,** 2 fold more FoxO3a binding to the MnSOD promoter in AC5 KD cells compared with LacZ control cells, n=3. The data in panels **A – E** did not have a normal distribution and the appropriate statistical tests were used (see statistical analysis section), *$p<0.05$

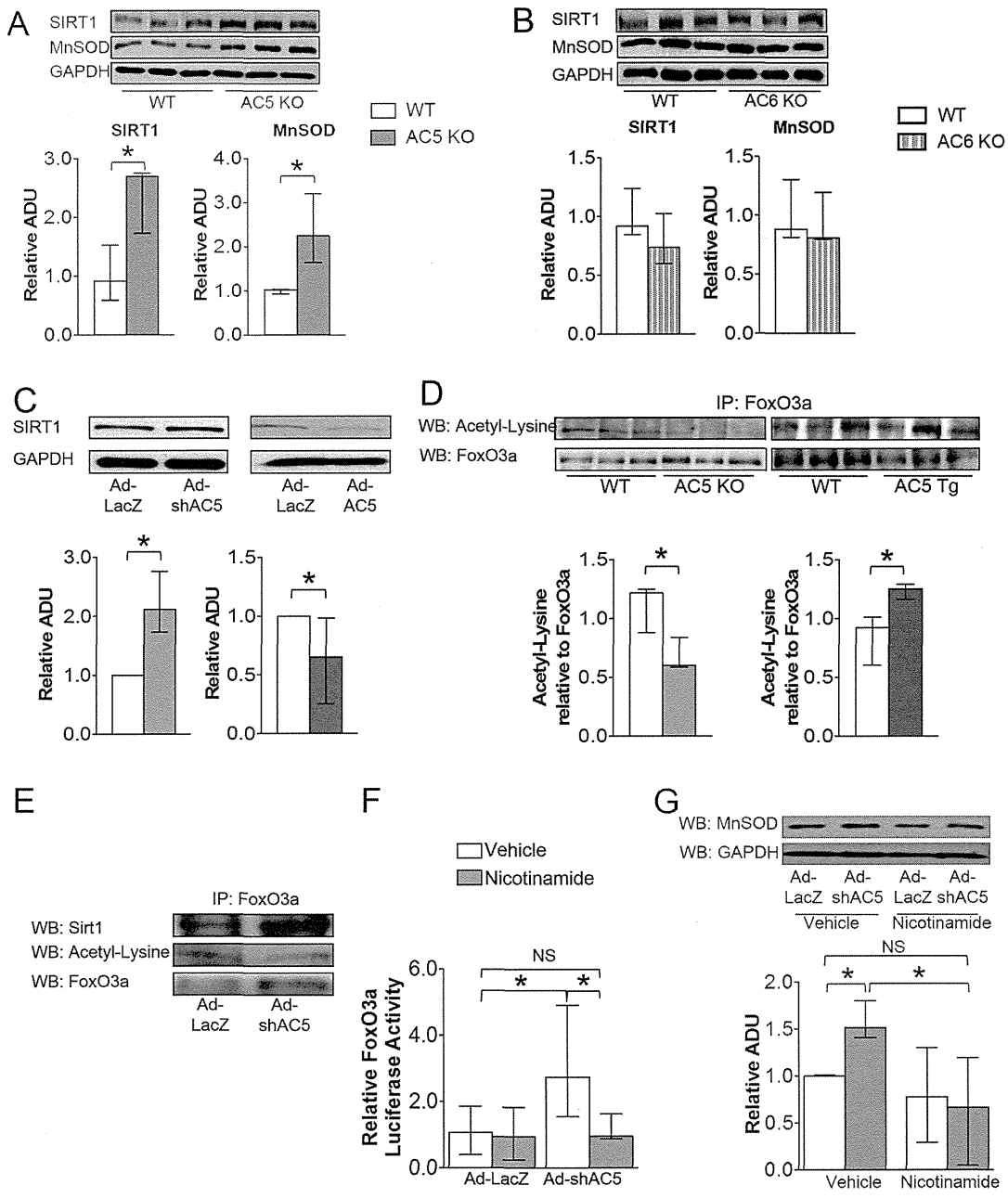

Figure 5.

AC5 regulated FoxO3a transcriptional activity through SIRT1. **A,** SIRT1 and MnSOD expression levels increased in AC5 KO heart, n=3/group, but not in AC6 KO hearts, n=3/group **(B)**. **C,** SIRT1 expression levels increased in AC5 KD cardiomyocytes (left panel) (n=4) and decreased in AC5 OE cardiomyocytes (right panel) (n=5). **D,** Acetyl-lysine in FoxO3a was down-regulated in AC5 KO mice heart (left panel), but up-regulated in AC5 Tg mouse heart (right panel), n=3/group. **E,** Co-IP confirmed that SIRT1 de-acetylated FoxO3a by directly binding to FoxO3a in AC5 KD cardiomyocytes. **F,** FoxO3a transcriptional activity was inhibited in AC5 KD myocytes treated with nicotinamide, a Sirtuin inhibitor,

n=9/group. The FoxO3a transcriptional activity of AC5 KD myocytes treated with nicotinamide showed no significant difference compared with cardiomyocytes infected with ad-LacZ, NS=non-significant. **G,** MnSOD expression level was inhibited in AC5 KD cardiomyocytes when the cells were treated with nicotinamide. n=6. The data in panels **A** – **G** did not have a normal distribution. The appropriate statistical tests are noted in the statistical analysis section. *$p<0.05$

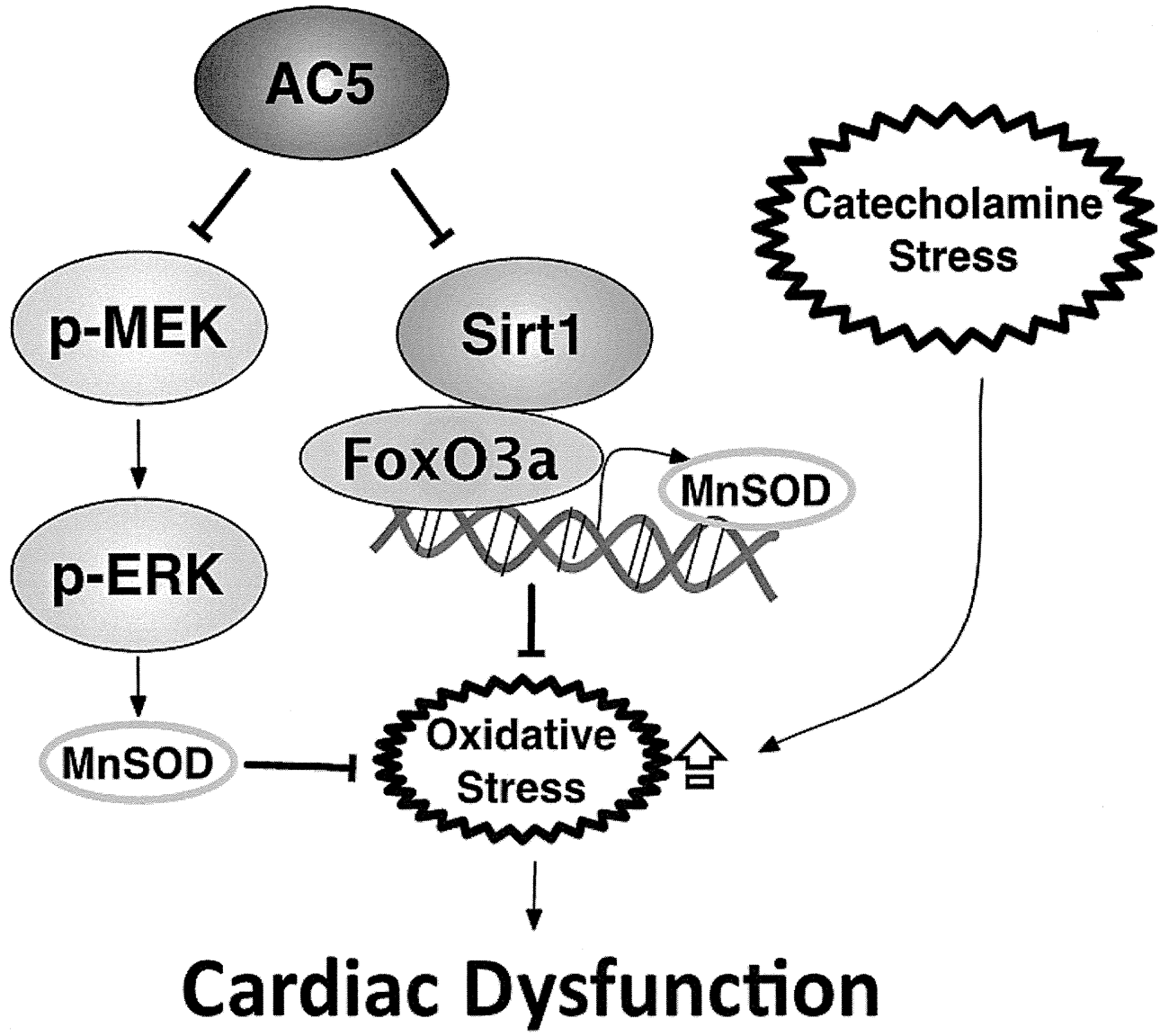

Figure 6.
Signaling diagram for AC5 regulation of MnSOD through the SIRT1/FoxO3a and the MEK/ERK pathway. Imbalance between reactive oxygen species production and the intracellular anti-oxidant system results in the intolerance of AC5 Tg to stress.

nature COMMUNICATIONS

ARTICLE

Received 23 Oct 2012 | Accepted 27 Feb 2013 | Published 9 Apr 2013

DOI: 10.1038/ncomms2673

OPEN

A role for Piezo2 in EPAC1-dependent mechanical allodynia

N. Eijkelkamp[1,2,†], J.E. Linley[1,†], J.M. Torres[1,3], L. Bee[1,4], A.H. Dickenson[4], M. Gringhuis[1], M.S. Minett[1], G.S. Hong[1,5], E. Lee[1,5], U. Oh[5], Y. Ishikawa[6], F.J. Zwartkuis[7], J.J. Cox[1] & J.N. Wood[1,5]

Aberrant mechanosensation has an important role in different pain states. Here we show that Epac1 (cyclic AMP sensor) potentiation of Piezo2-mediated mechanotransduction contributes to mechanical allodynia. Dorsal root ganglia Epac1 mRNA levels increase during neuropathic pain, and nerve damage-induced allodynia is reduced in Epac1 $-/-$ mice. The Epac-selective cAMP analogue 8-pCPT sensitizes mechanically evoked currents in sensory neurons. Human Piezo2 produces large mechanically gated currents that are enhanced by the activation of the cAMP-sensor Epac1 or cytosolic calcium but are unaffected by protein kinase C or protein kinase A and depend on the integrity of the cytoskeleton. *In vivo*, 8-pCPT induces long-lasting allodynia that is prevented by the knockdown of Epac1 and attenuated by mouse Piezo2 knockdown. Piezo2 knockdown also enhanced thresholds for light touch. Finally, 8-pCPT sensitizes responses to innocuous mechanical stimuli without changing the electrical excitability of sensory fibres. These data indicate that the Epac1-Piezo2 axis has a role in the development of mechanical allodynia during neuropathic pain.

[1] Molecular Nociception Group, Wolfson Institute for Biomedical Research, University College London, London WC1E 6BT, UK. [2] Laboratory of Neuroimmunology and Developmental Origins of Disease, University Medical Center Utrecht 3584 EA, The Netherlands. [3] Department of Biochemistry, Molecular Biology and Immunology, Faculty of Medicine, University of Granada, Granada 18012, Spain. [4] Research Department of Neuroscience, Physiology and Pharmacology, University College London, London WC1E 6BT, UK. [5] Department of Molecular Medicine and Biopharmaceutical Sciences, World Class University Program, Seoul National University, Seoul 151-742, South Korea. [6] Cardiovascular Research Institute, Yokohama City University Graduate School of Medicine, Yokohama 236-0004, Japan. [7] Department of Physiological Chemistry, University Medical Center Utrecht, Center for Biomedical Genetics and Cancer Genomics Center, Utrecht 3584 CG, The Netherlands. † There authors shared first authorship. Correspondence and requests for materials should be addressed to J.N.W. (email: J.Wood@ucl.ac.uk) or to N.E. (email: N.Eijkelkamp@umcutrecht.nl).

Sensory neurons innervate peripheral tissues where they transduce and transmit information about noxious and innocuous stimuli to the central nervous system[1,2]. Damage to sensory neurons as a result of chemotherapy, trauma or in diabetics and human immunodeficiency virus-infected patients may lead to neuropathic pain, often associated with mechanical allodynia, where normally innocuous stimuli such as light touch are perceived as painful[3]. The possible involvement of mechanotransducers such as Piezo or TRPC channels in the development of allodynia is a topic of interest[4,5].

Cyclic AMP is an intracellular signalling messenger that changes pain thresholds[6] through the activation of two sensors: protein kinase A (PKA) and Epac (exchange protein directly activated by cAMP)[7]. Intradermal injection of a cAMP analogue causes hypersensitivity to mechanical stimuli[6]. Importantly, mechanical allodynia in murine neuropathic pain models is severely attenuated in mice in which different adenylate cyclases, the enzyme family that generates cAMP, are genetically or pharmacologically targeted[8,9]. Interestingly, however, the downstream cAMP-sensor PKA is not required for the development of allodynia in neuropathic pain models[10,11]. The role of the cAMP-sensor Epac in the development of neuropathic pain-associated allodynia is unknown. Epac1 and Epac2 are guanine nucleotide exchange factors that activate Rap, a small GTP-binding protein of the Ras family of GTPases. The binding of cAMP or the Epac-specific agonist, 8-pCPT, stimulates Rap1 via the exchange of GDP for GTP[12,13]. Various effector proteins, including adaptor proteins that affect the cytoskeleton, regulators of G proteins of the Rho family, and phospholipases (for example, PLCε) and protein kinases, signal downstream from Rap[14].

Here we investigated the role of Epac signalling in the development of allodynia associated with neuropathic pain and the role of Piezo2 in this process. We show that the cAMP-sensor Epac1 sensitizes Piezo2 leading to allodynia. This work highlights a new pain pathway, which if successfully targeted, could potentially lead to better treatments for aspects of neuropathic pain.

Results

Epac1 expression in sensory neurons during neuropathic pain. We measured Epac1 and Epac2 mRNA expression in a neuropathic pain model. Four weeks after a unilateral L5 nerve transection (L5 SNT), mice displayed mechanical allodynia in the ipsilateral paw. Thresholds to mechanical stimulation were unaffected in contralateral paws, sham-operated mice or in naive untreated mice (Fig. 1a). At this time point, Epac1 mRNA levels in dorsal root ganglia (DRG) innervating the ipsilateral paw increased in comparison with DRG innervating the contralateral paw, from sham-operated animals, or from untreated mice by ~1.8-fold (Fig. 1b). Epac2 mRNA expression levels in DRG innervating the ipsilateral or contralateral paw were similar to Epac2 expression levels in DRG from sham-operated animals or naive untreated animals (Fig. 1c). The increase in Epac1 mRNA levels in the DRG innervating the ipsilateral paw was also observed at the protein level (Fig. 1d).

Epac1-dependent allodynia in neuropathic pain. Next we investigated whether Epac1 has a role in the development of allodynia in an L5 SNT neuropathic pain model. Epac1 protein levels were absent in DRG of *Epac1* −/− mice, while Epac1 protein levels were reduced by ~50% in *Epac1* +/− mice compared with wild-type (WT) mice (Fig. 1e). In control WT mice, spinal nerve transaction (SNT) induced mechanical allodynia that was present from day 1 after the operation and had fully developed in ~6 days. In mice completely deficient for Epac1 ($n=13$), SNT-induced allodynia was greatly attenuated compared with WT mice ($P<0.001$; $n=10$; two-way analysis of variance) or *Epac1* +/− mice ($P<0.001$; $n=10$; two-way analysis of variance) from day 1 (Fig. 1f). The magnitude of allodynia in *Epac1* +/− mice was also reduced compared with WT littermates ($P<0.05$; $n=10$; two-way analysis of variance) using repeated measures analysis (Fig. 1f). Overall these data indicate Epac1 is required for the development of allodynia in a mouse model of chronic neuropathic pain.

Epac signalling enhances sensory neuron mechanotransduction. Sensory neurons are intrinsically mechanosensitive and different types of mechanically gated current can be identified in the cell bodies of sensory neurons *in vitro*[15,16]. Neurons associated with detection of touch express low threshold rapidly adapting (RA) mechanically gated currents[2]. We asked whether activation of the cAMP-sensor Epac leads to changes in mechanically evoked RA currents in DRG neurons? Large diameter neurons (>35 μm) with fast action potentials (width of action potential <1 ms) were mechanically distended[17]. Application of the Epac-selective cAMP analogue 8-pCPT shifted the stimulus response curves of mechanically evoked RA currents to the left, resulting in increased currents in response to mechanical stimuli (~2-fold increase in inward current at a stimulus intensity of 12 μm) (Fig. 2a,d). 8-pCPT time dependently enhanced mechanically activated peak currents evoked by a ~12.5-μm distension that plateaued after ~15 min (Fig. 2b,d). Finally, 15 min after application of 8-pCPT the threshold of activation of RA currents was reduced by ~24% (Fig. 2c). Application of vehicle did not have any effect on mechanically evoked current sizes (Fig. 2).

Characterization of human Piezo2. DRG neurons in culture express at least three types of cation currents evoked by mechanical stimulation[16–18]. Piezo2 is expressed in mouse sensory neurons[4], and Piezo2 short interfering RNA application to sensory neuron cultures results in a ~75% loss of neurons expressing mechanically evoked RA currents[4]. As the Epac-specific cAMP analogue sensitized mechanically evoked RA currents, we first cloned human PIEZO2 (hPiezo2) cDNA into a mammalian expression vector, transfected it into HEK293 cells and characterized its biophysical properties by whole-cell voltage clamp. hPiezo2 currents activated within ~1 ms of the mechanical stimulus and were weakly outwardly rectifying (Fig. 3a) with a reversal potential of 9.7 ± 1.6 mV ($n=7$). hPiezo2 currents showed rapid adaptation to the mechanical stimulus which was voltage dependent, being 7-fold faster at negative holding voltages than positive holding voltages (V_{hold} −80 mV, Tau = 4.4 ± 0.8 ms; V_{hold} +80 mV, Tau = 29.4 ± 3.5 ms; $n=7$; $P<0.001$; *t*-test). Mechanically stimulating hPiezo2-expressing HEK293 cells at a rate of 1 Hz resulted in a rapid decay in the size of the mechanically evoked current (Supplementary Fig. S1a,b), similar to native rapidly adapting (RA) currents in DRG[19]. We next investigated the pharmacology of hPiezo2 (Fig. 3b–d). Acute bath addition of FM1-43, a permeant inhibitor of rapidly adapting mechanosensitive channels in sensory neurons[20], inhibited hPiezo2 currents (Fig. 3b–d). By contrast preincubation with dihydrostreptomycin, a blocker of the cochlear mechanotransducer channel[21], had no effect on either the magnitude or threshold of hPiezo2 currents (Fig. 3e,f).

Further characterization of hPiezo2 showed that mechanically evoked peak currents were directly proportional to probe velocity (Supplementary Fig. S1c,d), with decreased probe velocity resulting in smaller mechanically evoked currents. The

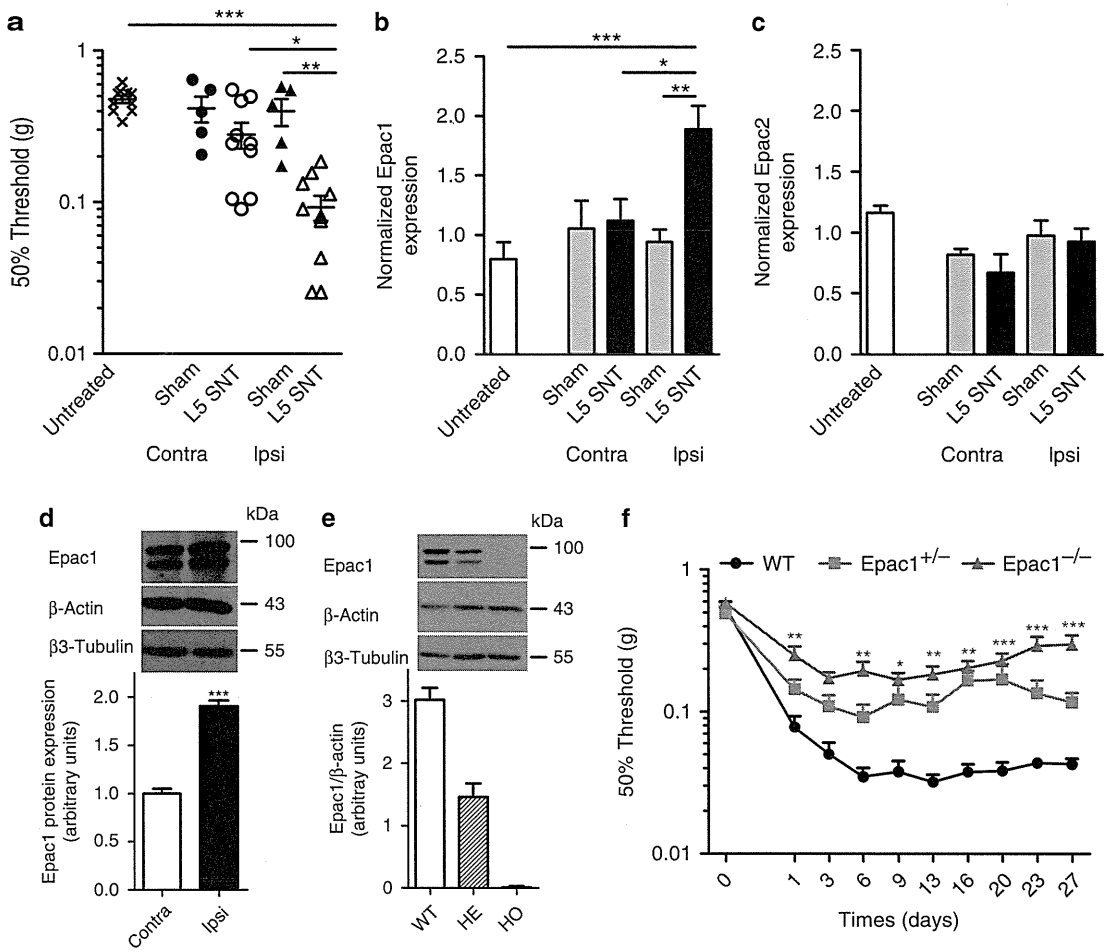

Figure 1 | DRG Epac1 expression is increased in and required for L5 spinal nerve transaction-induced allodynia. (**a**) The sensitivity to mechanical stimulation was determined in sham-operated mice ($n=5$), naive controls ($n=10$) or mice subjected to unilateral L5 SNT 4 weeks after surgery ($n=10$). Line with error bars represent mean ± s.e.m. (**b**) Epac1 or (**c**) Epac2 mRNA levels in DRGs innervating the contralateral (contra) or ipsilateral (ipsi) side of sham-operated, naive controls and L5 SNL mice 4 weeks after surgery. Epac1/2 mRNA expression levels were corrected for GAPDH and β-actin mRNA expression levels. (**d**) Epac1 protein expression levels in ipsilateral (affected) and contralateral (unaffected) DRGs of mice subjected to unilateral L5 SNT 4 weeks after surgery. β-Actin and the neuron-specific β3-tubulin was used as loading control. (**e**) Epac1 protein expression in DRGs of WT ($n=6$), Epac1+/− (HE, $n=4$) and Epac1−/− (HO, $n=4$) mice. (**f**) The sensitivity to mechanical stimulation was determined in wild-type ($n=10$), *Epac1*+/− ($n=10$) and *Epac1*−/− ($n=13$) mice subjected to unilateral L5 SNT. Repeated measures one-way analysis of variance (ANOVA) showed a significant genotype effect $F(2,30)=25{,}935$, $P<0.001$. Bonferoni *post hoc* analysis showed a significant effect between *Epac*−/− and WT ($P<0.001$); *Epac1*−/− and *Epac1*+/− ($P<0.001$); and *Epac1*+/− and WT ($P<0.05$). All data are expressed as mean ± s.e.m. (**a–c**) Data are analysed by ANOVA followed by the Bonferroni *post hoc* test. (**d**) Data are analysed using *t*-test. $^{*}P<0.05$, $^{**}P<0.01$, $^{***}P<00.1$.

biophysical properties of hPiezo2 are similar to those described for mouse Piezo2 and endogenous RA mechanosensitive currents expressed in large and small diameter DRG neurons[4,16,18]. Cytoskeletal elements have previously been shown to be essential for normal mechanotransduction in sensory neurons[16,22]. Preincubation of HEK293 cells overexpressing hPiezo2 with the actin depolymerizing agent latrunculin A strongly shifted the stimulus–response curve to the right resulting in a reduction in mechanical sensitivity of hPiezo2 (Supplementary Fig. S1e). Latrunculin A increased the threshold for activation ~5-fold (control: 2.4 ± 0.5 μm; lantruculin: 12.3 ± 1.2 μm, $P<0.001$; $n=6$–7; *t*-test). The microtubule depolymerizing agent colchicine reduced hPiezo2 peak currents in response to mechanical stimuli ≥7 μm (Supplementary Fig. S1f). However, no shift in the stimulus–response curve or change in mechanical threshold (control: 3.3 ± 0.5 μm; colchicine: 4.2 ± 0.4 μm; $P=0.15$; $n=16$; *t*-test) was observed. These findings indicate that the actin and tubulin cytoskeletons regulate hPiezo2 via distinct mechanisms.

Epac1 signalling enhances Piezo2-mediated mechanotransduction. As Epac signalling sensitizes mechanically evoked RA currents, we also tested effects on Piezo2-mediated mechanically evoked currents. We used HEK293a cells expressing Piezo2 and Epac1 or Epac2 (HEK293a cells express very low levels of Epac1/2) and mechanically distended these cells. Coexpression of Epac1 with Piezo2 in HEK293 cells did not change the stimulus–response curve compared with expression of Piezo2 alone (Fig. 4a). However, the addition of Epac-selective 8-pCPT to cells expressing Piezo2 and Epac1 strongly shifted the stimulus–response curve to the left. At a distension of ~8 μm, currents increased by ~2.5-fold (Fig. 4a,e). Coexpression of Epac2 with Piezo2 or application of 8-pCPT to cells expressing

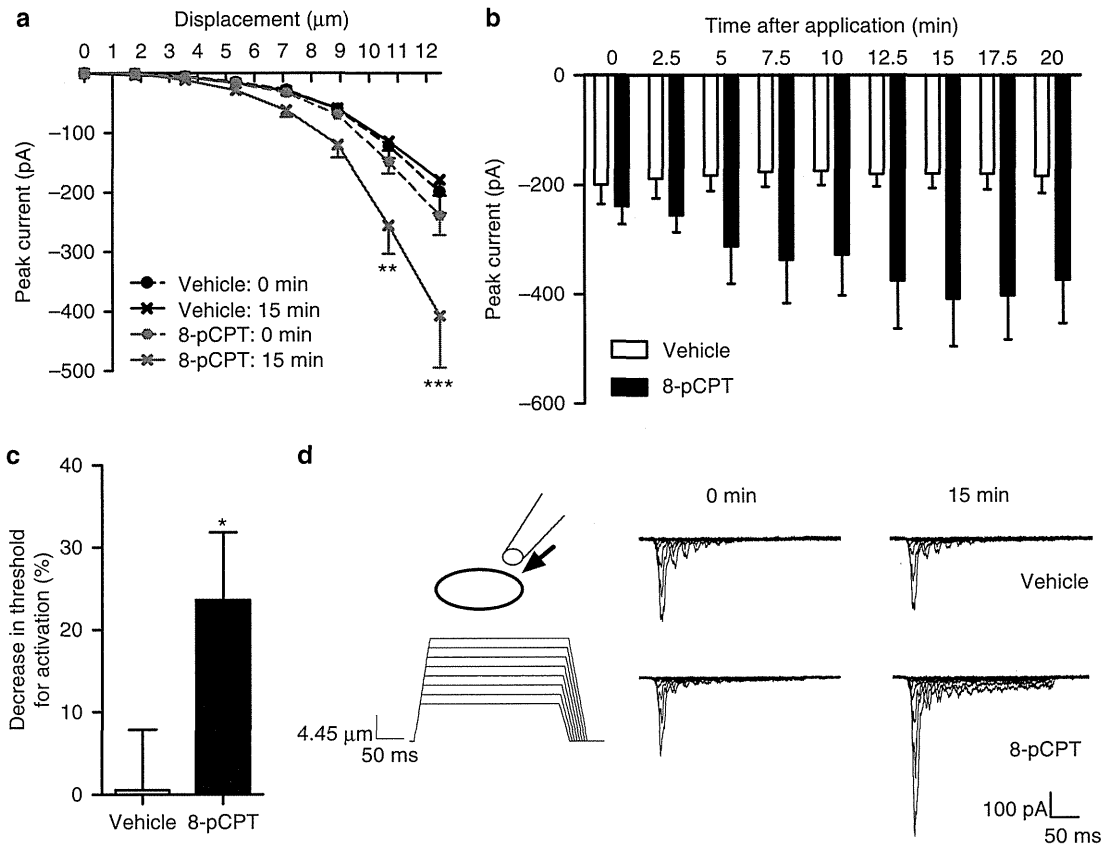

Figure 2 | 8-pCPT enhances rapidly adapting mechanically evoked currents in large diameter sensory neurons. (**a**) Stimulus-response curve of rapidly adapting currents evoked by mechanical stimulation before and 15 min after 8-pCPT or vehicle administration (vehicle, $n=13$; 8-pCPT, $n=17$). (**b**) Time course of peak currents evoked by a ~12.5-μm membrane deflection after administration of 8-pCPT into the bath solution. Repeated measures one-way analysis of variance: time, $P<0.05$; treatment, $P>.05$; interaction: $P<0.01$ ($n=14$). (**c**) Threshold of activation was determined as mechanical stimulus that elicited a current >20 pA. The decrease in threshold of activation after 8-pCPT was calculated as percentage of baseline thresholds. (**d**) Representative example of whole-cell voltage clamp traces from a large diameter mouse DRG neuron with a narrow action potential width in response to increasing membrane deformation (holding potential −60 mV) before and after 8-pCPT or vehicle administration. All data are expressed as mean ± s.e.m. (**a–b**) Data were analysed using two-way analysis of variance followed by the Bonferroni *post hoc* test. (**d**) Data are analysed by *t*-test. $^*P<0.05$, $^{**}P<0.01$, $^{***}P<0.001$.

Piezo2 + Epac2 or Piezo2 alone did not change the stimulus–response curve (Fig. 4b). In Epac1 expressing cells, 8-pCPT also increased the maximal mechanically evoked inward current before whole-cell configuration was lost because of the strength of the mechanical stimulus and reduced the threshold of activation, whereas Epac2 had no effect on either parameter (Fig. 4c,d). In cells expressing hPiezo1 and Epac1, 8-pCPT-induced activation of Epac1 also shifted the stimulus response of mechanically evoked Piezo1 currents to the left and decreased thresholds of activation, whereas no effect was seen when Epac2 was coexpressed with hPiezo1 (Supplementary Fig. S2). Overall these data indicate that Epac1 but not Epac2 activation results in sensitization of mechanically evoked Piezo-dependent currents. We further tested whether activation of other signalling molecules known to be involved in the development of mechanical hypersensitivity such as PKA, protein kinase C (PKC) and Ca^{2+} sensitize Piezo2 currents. Increasing cytosolic Ca^{2+} from 50 nM to 1 μM in Piezo2 expressing HEK293 cells resulted in sensitization of the mechanically evoked current (Supplementary Fig. S3a,b) and a reduction in threshold for channel activation (Supplementary Fig. S3c). Elevating cytosolic calcium also produced a marked slowing of adaptation to the static mechanical stimulus at cell displacements ≥4 μm (Supplementary Fig. 3d). In contrast, activation of PKC by preincubation with the phorbol derivative PMA had no effect on hPiezo2 channel activity or threshold (Supplementary Fig. S3e,f). Similarly, activation of PKA by preincubation with 6-Bnz-cAMP, a selective agonist of PKA, which does not activate Epac, had no significant effect on the stimulus–response curve (Supplementary Fig. S3g,h).

Epac activation causes long-lasting mechanical allodynia. 8-pCPT has been shown to cause increased sensitivity to noxious mechanical stimuli (hyperalgesia)[23]. Activation of the cAMP-sensor PKA, induces hyperalgesia through effects on excitability, but not through sensitizing mechanotransduction[1]. We tested whether selective activation of Epac increased sensitivity to touch and compared this with the development of mechanical hypersensitivity induced by a PKA-selective cAMP analogue (6-Bnz-cAMP). Intraplantar injection of either 6-Bnz-cAMP or 8-pCPT dose-dependently (12.5 pmol per paw–12.5 nmol per paw) induced mechanical hypersensitivity that increased in magnitude and duration with increasing doses (Fig. 5a,b). At every dose tested, the magnitude of 6-Bnz-cAMP and 8-pCPT-induced mechanical hypersensitivity was statistically indistinguishable